

# THE MECHANICS OF RUNNING: HOW DOES STIFFNESS COUPLE WITH SPEED?

THOMAS A. McMAHON and GEORGE C. CHENG

Division of Applied Sciences, Harvard University, Cambridge, MA 02138, U.S.A.

**Abstract**—A mathematical model for terrestrial running is presented, based on a leg with the properties of a simple spring. Experimental force–platform evidence is reviewed justifying the formulation of the model. The governing differential equations are given in dimensionless form to make the results representative of animals of all body sizes. The dimensionless input parameters are:  $U$ , a horizontal Froude number based on forward speed and leg length;  $V$ , a vertical Froude number based on vertical landing velocity and leg length, and  $K_{\text{LEG}}$ , a dimensionless stiffness for the leg-spring. Results show that at high forward speed,  $K_{\text{LEG}}$  is a nearly linear function of both  $U$  and  $V$ , while the effective vertical stiffness is a quadratic function of  $U$ . For each  $U, V$  pair, the simulation shows that the vertical force at mid-step may be minimized by the choice of a particular step length. A particularly useful specification of the theory occurs when both  $K_{\text{LEG}}$  and  $V$  are assumed fixed. When  $K_{\text{LEG}} = 15$  and  $V = 0.18$ , the model makes predictions of relative stride length  $S$  and initial leg angle  $\theta_0$  that are in good agreement with experimental data obtained from the literature.

## NOMENCLATURE

### Dimensional variables

$f_{\text{max}}$	maximum vertical force
$f_x$	horizontal force on mass
$f_y$	vertical force on mass
$k_{\text{leg}}$	spring stiffness of leg
$k_{\text{vert}}$	effective vertical stiffness (same as $k_{\text{leg}}$ in the case of vertical hopping; otherwise different)
$l$	instantaneous length of leg [Fig. 2(b)]
$l_0$	starting and ending leg length
$m$	body mass
$s$	stride length, distance between footprints of same foot
$2l_0 \sin \theta_0$	step length, distance moved during one contact period
$t_a$	time in air
$t_c$	time of contact
$u$	horizontal velocity at beginning of contact
$-v$	vertical velocity at beginning of contact
$x$	horizontal coordinate of body mass [Fig. 2(b)]
$y$	vertical coordinate of body mass [Figs 2(a) and (b)]

### Dimensionless variables

$A_y = f_y/mg - 1$	dimensionless vertical acceleration
$K_{\text{LEG}} = k_{\text{leg}}l_0/mg$	dimensionless leg stiffness
$K_{\text{VERT}} = k_{\text{vert}}l_0/mg$	dimensionless vertical stiffness
$L = l/l_0$	dimensionless leg length
$S = s/l_0$	relative stride length
$U = u/(gl_0)^{1/2}$	horizontal Froude number
$V = v/(gl_0)^{1/2}$	vertical Froude number
$t\omega_0/g = K_{\text{VERT}}^{1/2}V$	Groucho number

## INTRODUCTION

This paper presents a simple yet comprehensive theory for running in terrestrial animals. We first review experimental evidence justifying our main assumption, that the leg is a spring. Then we give a series of results predicting important parameters such as the

peak ground reaction force and the stride length. Finally, we compare these predictions with published experiments. We seek the simplest model of running capable of explaining how the stiffness of the leg spring couples with speed. Before beginning, however, it is useful to ask an even more basic question: what distinguishes walking and running?

At first glance, the difference between walking and running in terrestrial animals would appear obvious. In running, all feet are in the air at some point in the gait cycle, whereas in walking there is always at least one foot on the ground. This distinction is appropriate most of the time for most animals, but there are times when it fails. When humans run along a circular path, the aerial phase of the motion disappears if the turn has a sufficiently small radius (Greene and McMahon, 1979a). When humans run on a treadmill at constant speed but deliberately bend their knees more than usual in order to decrease the vertical stiffness of the legs and body, again the aerial phase is found to disappear when the extra knee flexion is great enough (McMahon *et al.*, 1987).

A better criterion for distinguishing between walking and running is the one put forward by Cavagna *et al.* (1976). On the basis of observations in humans, they pointed out that in walking, the center of mass is highest in mid-step, when the hip of the stance leg passes over the ankle. In running, by comparison, the center of mass is lowest at mid-step. Thus in walking, but not in running, gravitational potential energy is stored in the first half of the walking step as the center of mass rises, and returned in the form of kinetic energy during the second half of the step as the center of mass falls.

Cavagna *et al.* (1976) emphasized that in running, changes of forward kinetic energy and gravitational potential energy are in phase and therefore cannot exchange with one another to smooth out fluctuations

of total mechanical energy over a step. They pointed out, however, that energy can still be stored at mid-step in an elastic form within stretched tendons, muscles, and perhaps bent bones. These general features of walking and running were later recognized in the gaits of birds and quadrupedal mammals as well as humans (Cavagna *et al.*, 1977).

In this paper, our most important goal is to understand the quantitative rules that couple leg-spring stiffness, gravity, and forward speed in running. We also wish to know the relationship between the leg-spring stiffness and the equivalent vertical stiffness, a parameter that is easy to measure in running animals. In order to make the results of the paper valid for animals of all body size, the model is formulated in terms of dimensionless variables.

## METHODS

### Justification of the model

In Fig. 1, reproduced from Cavagna *et al.* (1988), the spring-like properties of the limbs in running are illustrated for a dog trotting, a man running, and a kangaroo hopping. These records, obtained as each animal ran at constant speed over a force platform, show that the vertical acceleration (and thus the vertical force) increases as the vertical displacement of the center of mass decreases during the period of contact. Furthermore, the portions of the curves showing loading of a hypothetical spring (leftward arrow) and unloading (rightward arrow) nearly coincide, at least for the dog and the kangaroo, supporting

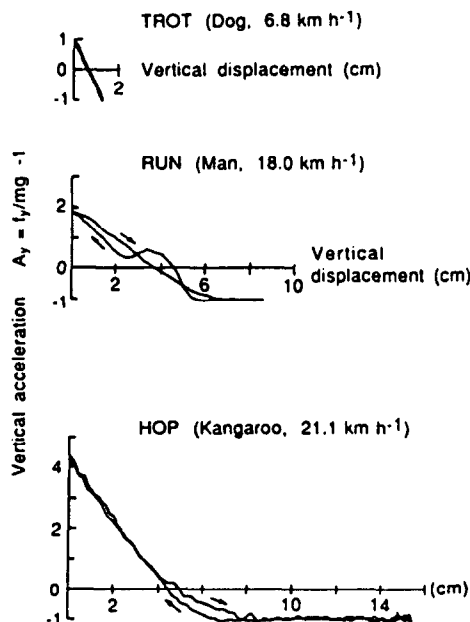


Fig. 1. Vertical acceleration vs vertical displacement for a 5 kg dog trotting, a 72 kg man running, and a 21 kg kangaroo hopping across a force platform at the steady speeds shown. From Cavagna *et al.* (1988).

the idea that the same undamped spring can describe the stiffness of a running animal during the entire contact period.

As a model of an animal hopping in place, imagine that the leg is a linear spring and the body mass falls on it with a certain downward vertical velocity. Provided that the spring is undamped, the vertical velocity is reversed during the collision. The stiffer the spring, the shorter the contact time and the higher the peak vertical force. Now let the animal run forward. A steady running cycle will be obtained if in each collision with the ground the forward speed is the same at the beginning and the end of the step. During the collision, the vertical velocity is reversed and the magnitude of the angle between the leg and the vertical is the same at the end of the step as it was at the beginning. For a given set of values for the body mass, the (unloaded) leg length, the horizontal and vertical landing velocities, the initial angle of the leg, and gravity, only one particular value of the spring constant for the leg-spring will do. If the leg-spring is too hard, the body will fly upward too soon, and if the leg-spring is too soft, the body will rise too late.

In the following sections, two alternative schemes are considered for putting the problem of the rebound of a mass from a spring in dimensionless terms. The first applies to hopping in place, the second to forward running.

### Formulation of the model

**Hopping in place.** Figure 2(a) shows a mass-spring system constrained to move vertically as it strikes the ground. For reasons which will become clear later in the paper, we label the stiffness of the leg-spring  $k_{\text{vert}}$ . For vertical hopping, the terms  $k_{\text{leg}}$  and  $k_{\text{vert}}$  are

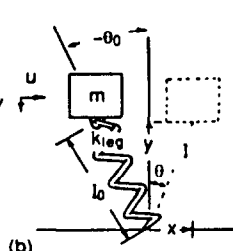
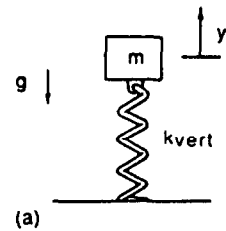


Fig. 2. Schematic diagrams showing (a) hopping in place, with no forward motion; and (b) hopping or running forward.

identical and may be used interchangeably. The displacement  $y$  of the mass is measured such that  $y$  is increasing when the mass is moving upward. The spring is slack, neither stretched nor compressed, when  $y=0$ . The vertical velocity  $dy/dt$  of the mass at the moment the leg-spring strikes the ground is  $-v$ , where  $v$  is a positive quantity. When  $y$  is made dimensionless by multiplying by  $k_{\text{vert}}/mg$  (where  $m$  is the mass, and  $g$  is the acceleration due to gravity) and when time is made dimensionless by multiplying by  $\omega_0 = (k_{\text{vert}}/m)^{1/2}$ , the equation of motion takes a particularly simple form. As shown in Appendix A, all the important performance measures, including the peak force the leg must bear, the time the leg spends in contact with the ground, and the stride frequency, depend on only one dimensionless group,  $v\omega_0/g$ . In a previous paper, where subjects changed the stiffness of their legs by running with their knees bent more than usual, the group  $v\omega_0/g$  was called the 'Groucho number' (McMahon *et al.*, 1987).

*Including the forward motion.* Several new variables enter the problem when the mass-spring model is extended to include forward motion. Suppose, as is shown in Fig. 2(b), the initial (zero-force) length of the leg is  $l_0$  and it has a stiffness of  $k_{\text{leg}}$ . In this formulation,  $y$  still measures the vertical height of the mass, but now  $y=0$  corresponds to the ground plane.

At the beginning of the rebound, the forward velocity  $dx/dt$  of the mass is  $u$  and the vertical velocity  $dy/dt$  is  $-v$ . During the rebound, we assume that the angle of the leg with respect to the vertical begins at  $-\theta_0$  and ends at  $+\theta_0$ . The  $x$ -velocity begins and ends with the value  $u$ , and the  $y$ -velocity is reversed by the step, starting with the value  $-v$  and ending with  $+v$ .

In Appendix B, the equations of motion and the initial and final conditions are given in a particular dimensionless form. Lengths have been normalized with respect to  $l_0$  and time has been made dimensionless by multiplying by the group  $(g/l_0)^{1/2}$ , which happens to be the (small-amplitude) frequency of a pendulum made by hanging the mass from the (unstretched) leg. As a consequence of substituting the assumed normalizations for length and time into the conditions on the initial and final velocities, an interesting thing happens [equations (B9)–(B11)]: the initial and final velocities are divided by a reference velocity  $(gl_0)^{1/2}$ . This reference velocity has a simple meaning. An inverted pendulum of length  $l_0$  swinging through the top of its arc would fly off the ground if the speed of its mass were greater than  $(gl_0)^{1/2}$ . In fluid mechanics, a velocity made dimensionless by the factor  $(\text{acceleration of gravity} \times \text{length})^{1/2}$  is called a Froude number (although some authors define  $v^2/gl_0$  as the Froude number).

Turning to equations (B1) and (B2), it is apparent that a single dimensionless parameter  $K_{\text{LEG}} = k_{\text{leg}}l_0/mg$  appears in the equations determining the motion of the mass after the initial moment. One way to interpret this ratio is to notice that the product

$k_{\text{leg}}l_0$  is the greatest force that the leg-spring can develop, i.e. the force in the spring when it has been compressed as far as it can go. Therefore, if the parameter  $k_{\text{leg}}l_0/mg < 1.0$ , the leg-spring cannot develop a force equal to the weight. If  $k_{\text{leg}}l_0/mg \ll 1.0$ , the mass follows a ballistic trajectory, one determined by the initial velocities and gravity only, after the initial moment. Another way to view the parameter  $k_{\text{leg}}l_0/mg$  is to recognize that it is the square of the ratio of the natural frequency of the mass-spring system to the natural frequency of the leg as a pendulum.

The different definition for  $y$  and the choices for reference lengths and times in Fig. 2(b) as opposed to 2(a) were made for clarity in the forms of the resulting dimensionless equations. As must be true, equation (B2) becomes equation (A1) in the limit of  $\theta = 0$ , employing definitions (A2), (A3), (B3) and (B4). Furthermore, in the limit of  $\theta = 0$ , one equation disappears (B1), one dimensionless group disappears ( $U = 0$ ), and the solution depends only on the Groucho number  $v\omega_0/g = K_{\text{VERT}}^{1/2} V$ .

#### Numerical methods

Because equations (B1) and (B2) are nonlinear, they must be solved subject to the conditions (B6)–(B11) using numerical integration procedures. The equations and their initial and final conditions constitute a two-point boundary value problem that was solved using a shooting method.

A fourth order Runge-Kutta algorithm was employed to integrate (B1) and (B2) forward in time steps of  $5 \times 10^{-5}$  dimensionless units [defined in equation (B4)]. Halving the time step produced no change in the results for a trajectory (to four significant places). Beginning with specified values for  $U = u/(gl_0)^{1/2}$ ,  $V = v/(gl_0)^{1/2}$ , and  $\theta_0$ , plus an initial choice for  $K_{\text{LEG}} = k_{\text{leg}}l_0/mg$ , the equations were integrated forward in time as the leg compressed and re-extended until it returned back to full extension ( $L = l/l_0 = 1.0$ ). If the final leg angle was greater than  $\theta_0$ , the procedure was repeated using a higher value for  $K_{\text{LEG}}$ ; if the final angle was less than  $\theta_0$ , the next approximation for  $K_{\text{LEG}}$  was smaller. The secant iteration technique (Press *et al.*, 1986) was used to estimate a new value for  $K_{\text{LEG}}$ . Iteration was discontinued and the solution accepted when the final angle for a trajectory was within  $10^{-4}$  radians of the magnitude of the starting angle and the final values for  $L$ ,  $U$ , and  $V$  were within one-hundredth of one per cent of the target end conditions.

## RESULTS

#### Trajectories and forces

Results for a typical simulation of running are shown in Fig. 3. The solid curves show results from the model when the input parameters were chosen to represent a man of average size (mass = 72 kg,

leg length = 1.0 m) running at a moderate speed ( $18.0 \text{ km h}^{-1}$ , between 5 and 6 min per mile). It is clear from Fig. 3(a) that the body mass reaches its lowest point midway through the step. The trajectory is rather flat; the body is only 6.24 cm lower in the middle of the step than it is at the beginning or the end. The vertical force reaches a maximum of 2.86 times body weight [Fig. 3(b)], while the peak negative and positive values of horizontal force are 0.554 times body weight [Fig. 3(c)].

In order to demonstrate the effect of changing just one input parameter, the broken curves in Fig. 3 show how the results are altered when the vertical landing velocity is reduced by about 60% while leaving the initial horizontal velocity and leg angle unchanged. The required leg-spring stiffness  $K_{\text{LEG}}$  declines from 15.5 to 13.6, the trajectory is flatter, the peak horizontal and vertical forces are smaller, and the dimensionless time occupied by the contact period increases.

#### Required leg stiffness

Following the example above, we systematically changed the input parameters, one at a time, covering the entire range of parameter space we judged relevant to vertebrate terrestrial locomotion. Results for the required leg-spring stiffness  $K_{\text{LEG}}$  are shown in Fig. 4. In part (a),  $K_{\text{LEG}}$  is plotted vs the dimensionless vertical velocity  $V$ , and it is apparent that  $K_{\text{LEG}}$  increases approximately linearly with  $V$  for the values of  $U$  investigated. Furthermore, as shown in part (b),  $K_{\text{LEG}}$  increases linearly with  $U$  in the range from  $U = 2$  to 10. The linear behavior continues in the range from  $U = 10$  to 30, although apparently this does not correspond to a range used by animals, and therefore does not appear in the plot. As shown in part (c),  $K_{\text{LEG}}$  declines with increasing initial leg angle for all values of  $U$ .

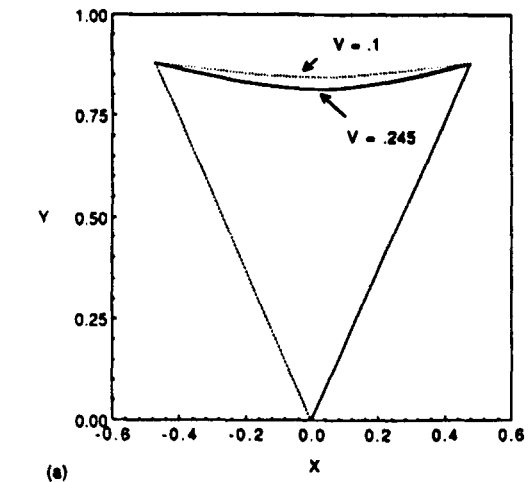
#### Peak vertical force

The dimensionless maximum vertical force  $f_{\text{max}}/mg$ , which occurs in the middle of the contact period, is plotted as a function of the input parameters in Fig. 5. This peak force rises linearly with  $V$  and  $U$  [Fig. 5(a)], but is a nonlinear function of  $\theta_0$  [Fig. 5(b)]. As shown in Fig. 5(b), there is a particular value of  $\theta_0$  (a different value of  $\theta_0$  for each combination of  $V$  and  $U$ ) at which  $f_{\text{max}}/mg$  is a minimum. The value of  $\theta_0$  that minimizes  $f_{\text{max}}/mg$  is plotted as a function of  $U$  in Fig. 5(c) for several values of  $V$ .

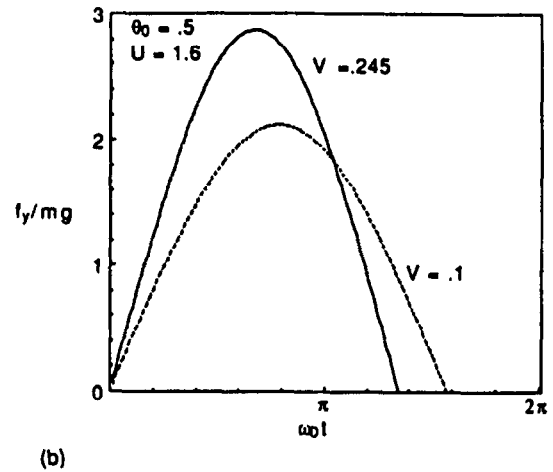
Since the force is maximum at the same moment that the length of the leg reaches a minimum (at mid-step), the height of the mass may be calculated at mid-step from

$$L_{\text{min}} = (l/l_0)_{\text{min}} = 1 - (f_{\text{max}}/mg)/K_{\text{LEG}}. \quad (1)$$

Using this calculation and the beginning and end conditions,  $L = 1$  at  $\theta = -\theta_0$  and  $\theta = \theta_0$ , it is possible to 'fair in' a curve between the three points, giving a



(a)



(b)

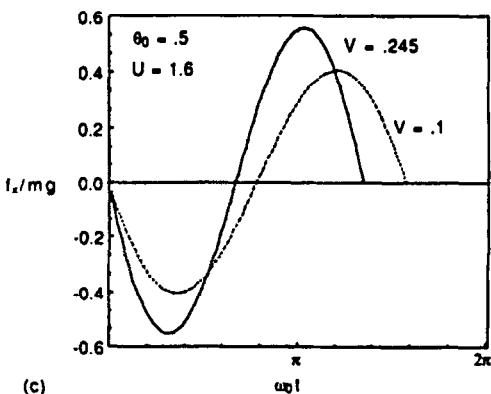
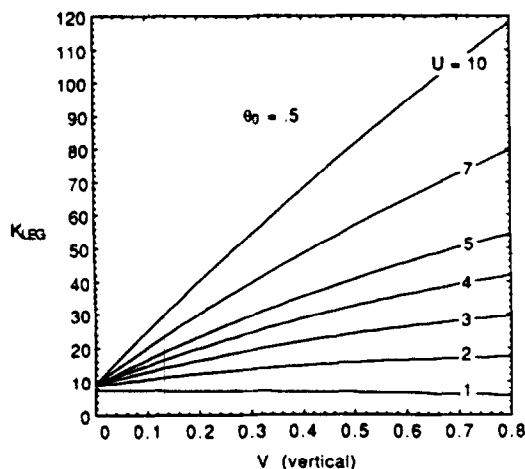
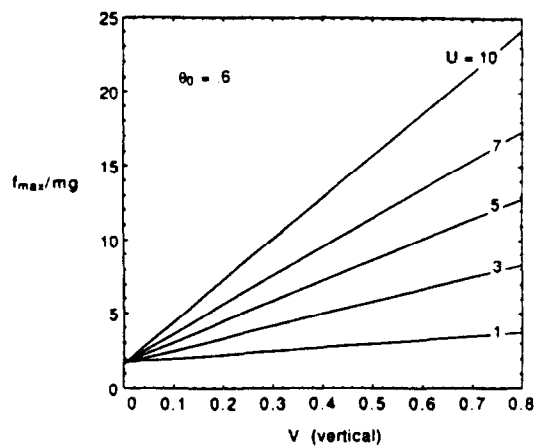


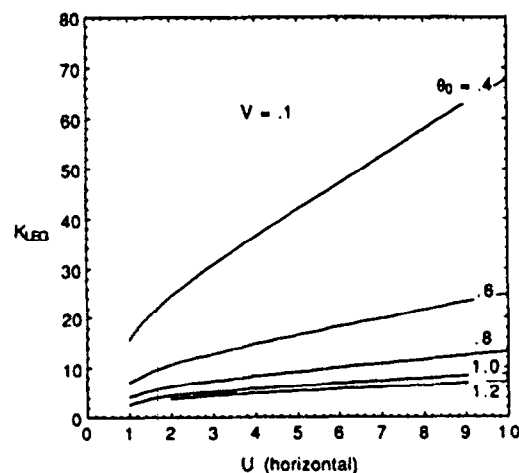
Fig. 3. Results when the input parameters represent the man running at  $18.0 \text{ km h}^{-1}$  ( $U = 1.6$ ,  $V = 0.245$ ,  $\theta_0 = 0.50$ ), contrasting the outcomes for two different dimensionless vertical velocities,  $V = 0.245$  and  $V = 0.1$ . (a) Trajectory of the mass; (b) dimensionless vertical force  $f_y/mg$  vs dimensionless time  $\omega_0 t$ ; (c) dimensionless horizontal force  $f_x/mg$  vs  $\omega_0 t$ .



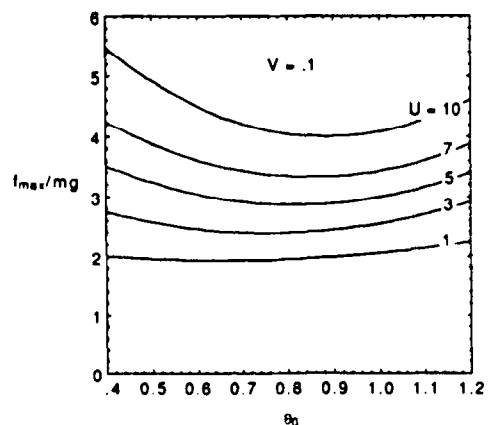
(a)



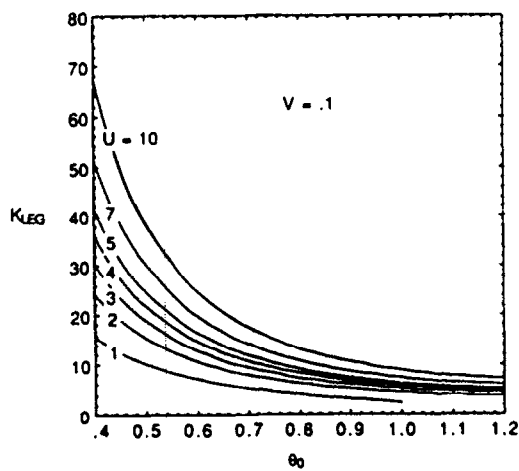
(a)



(b)

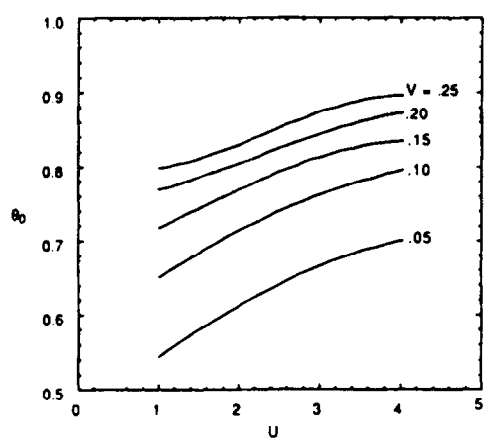


(b)



(c)

Fig. 4. Solutions showing dimensionless leg stiffness  $K_{LEG} = k_{leg}l_0/mg$  as a function of the input parameters. (a)  $V = v/(gl_0)^{1/2}$ ; (b)  $U = u/(gl_0)^{1/2}$ ; (c)  $\theta_0$ .



(c)

Fig. 5. Dimensionless peak vertical force at mid-step  $f_{max}/mg$  vs (a)  $V$  and  $U$ ; (b)  $\theta_0$  and  $U$ ; (c) results showing the  $\theta_0$  required to minimize  $f_{max}/mg$  as a function of  $U$  and  $V$ .

reasonable approximation of the trajectory followed by the mass during contact.

#### Vertical force vs displacement curves

A particularly useful set of results from the model is shown in Fig. 6, where the normalized vertical acceleration of the mass  $A_y = f_y/mg - 1$  is plotted against the vertical displacement  $\Delta y$ . The three parts of the figure, which are to be compared with the experimental records in Fig. 1, show simulations of: (a) a 5.0 kg dog trotting at  $6.8 \text{ km h}^{-1}$ ; (b) a 72 kg man running at  $18.0 \text{ km h}^{-1}$ ; and (c) a 21 kg kangaroo hopping at  $21.1 \text{ km h}^{-1}$ . The values assumed for the leg length and the input parameters  $U$ ,  $V$ , and  $\theta_0$  for each simulation are given in Table I.

The following procedure was used to obtain the best simulation of each experimental situation. Firstly, the change in vertical displacement of the center of mass during the aerial phase was read from Fig. 1, and the vertical landing velocity was calculated. From the leg length,  $U$  and  $V$  could now be fixed. Assuming that the step length was approximately equal to the leg length, a trial value could be obtained for  $\theta_0$ . Iterations were performed on  $\theta_0$  until the peak value for  $f_y/mg$  and the change in vertical displacement during the contact period came close to the experimental values available from Fig. 1.

#### Vertical stiffness

In Fig. 6, the portions of the curves corresponding to the contact period are generally linear (although the one simulating the man is straighter than those for the dog and kangaroo). From Fig. 6(b) (for the man) it is reasonable to propose an 'effective vertical stiffness', or just 'vertical stiffness'. One way to estimate the vertical stiffness is to divide the peak change in vertical force by the change in vertical displacement during contact (alternative methods will be mentioned in the Discussion section). Using this method, the dimensionless vertical stiffness may be calculated from

$$K_{\text{VERT}} = k_{\text{vert}} l_0 / mg = (\Delta f_y / \Delta y) l_0 / mg. \quad (2)$$

When this is done for Fig. 6(b), the result is  $K_{\text{VERT}} = 45.86$ . Both  $K_{\text{VERT}}$  and the actual normalized stiffness of the leg-spring  $K_{\text{LEG}}$  are plotted as a function of  $U$  in Fig. 7(a). It is clear that  $K_{\text{VERT}}$  is greater than  $K_{\text{LEG}}$ . For example, at  $U = 1.6$ , corresponding to the man running at  $18.0 \text{ km h}^{-1}$ , the ratio  $K_{\text{VERT}}/K_{\text{LEG}} = 45.86/15.49 = 2.96$ . At higher values of  $U$ ,  $K_{\text{VERT}}$  can be 5 or even 10 times greater than  $K_{\text{LEG}}$ .

Another difference between  $K_{\text{VERT}}$  and  $K_{\text{LEG}}$  is shown in parts (a) and (b) of Fig. 7. In Fig. 7(a), it is clear (as it was in Fig. 4(b), showing results from other simulations) that the required  $K_{\text{LEG}}$  for a re-entrant running cycle increases linearly with  $U$  for values of  $U$  greater than about 2.0. By comparison,  $K_{\text{VERT}}$  increases quadratically with  $U$  for values of  $U$  above about 2.0. This is demonstrated in Fig. 7(b), where a plot of  $K_{\text{VERT}}$  vs  $U^2$  follows an approximately straight line for values of  $U^2$  greater than about 4.0.

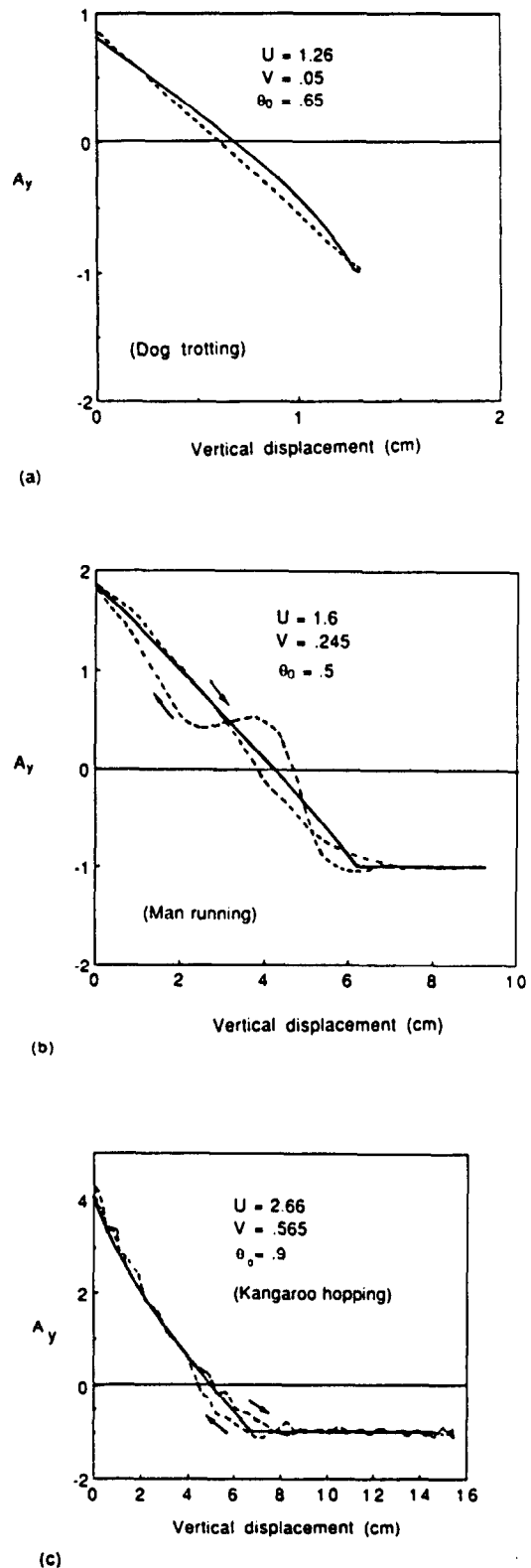


Fig. 6. Simulations of the running and hopping steps in Fig. 1, showing the results (solid curves) for the dimensionless vertical acceleration  $A_y = (f_y/mg - 1)$  vs vertical displacement for (a) the dog trotting; (b) the man running; (c) the kangaroo hopping. All input parameters for these simulations are summarized in Table I. The broken curves show the experimental results from Fig. 1, for comparison.

Table 1.

Animal	mass (kg)	$l_0$ (m)	$u$ (km h <sup>-1</sup> )	$U$	$V$	$\theta_0$
Dog	5.0	0.23	6.8	1.26	0.050	0.65
Man	72.0	1.00	18.0	1.60	0.245	0.50
Kangaroo	21.0	0.50	21.1	2.66	0.565	0.90

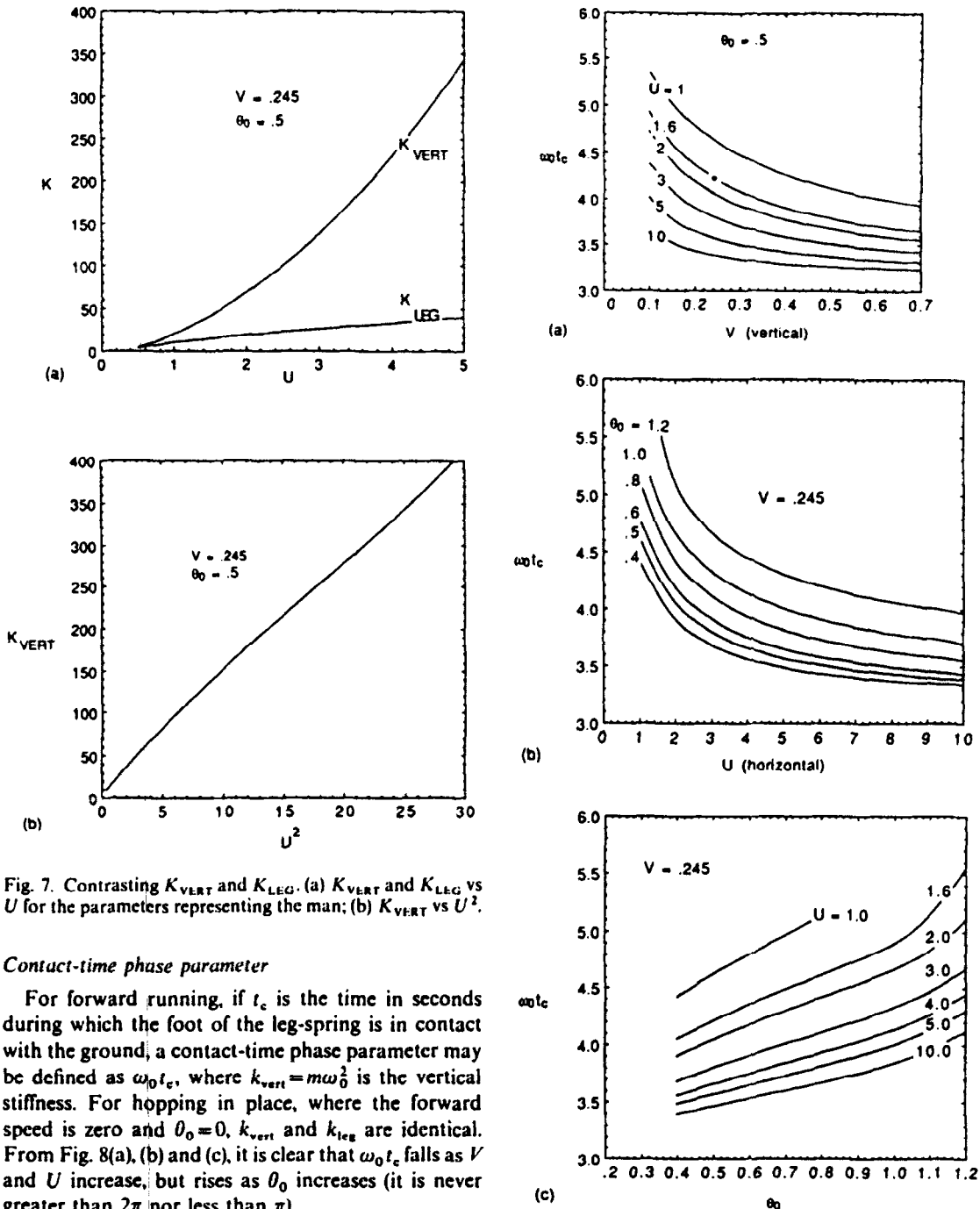


Fig. 7. Contrasting  $K_{\text{VERT}}$  and  $K_{\text{LEG}}$ . (a)  $K_{\text{VERT}}$  and  $K_{\text{LEG}}$  vs  $U$  for the parameters representing the man; (b)  $K_{\text{VERT}}$  vs  $U^2$ .

#### Contact-time phase parameter

For forward running, if  $t_c$  is the time in seconds during which the foot of the leg-spring is in contact with the ground, a contact-time phase parameter may be defined as  $\omega_0 t_c$ , where  $k_{\text{vert}} = m\omega_0^2$  is the vertical stiffness. For hopping in place, where the forward speed is zero and  $\theta_0 = 0$ ,  $k_{\text{vert}}$  and  $k_{\text{leg}}$  are identical. From Fig. 8(a), (b) and (c), it is clear that  $\omega_0 t_c$  falls as  $V$  and  $U$  increase, but rises as  $\theta_0$  increases (it is never greater than  $2\pi$  nor less than  $\pi$ ).

#### Stride length

In Appendix C, a derivation is given of a closed-form result relating the stride length to the input

Fig. 8. Dimensionless contact time  $\omega_0 t_c$  as a function of (a)  $V$ ; (b)  $U$ ; (c)  $\theta_0$ . Because the contact time is determined by the vertical motion,  $\omega_0 = (k_{\text{vert}}/m)^{1/2}$ . The star in (a) marks the result for the 72 kg man running at 18.0 km h<sup>-1</sup> (Table 1).

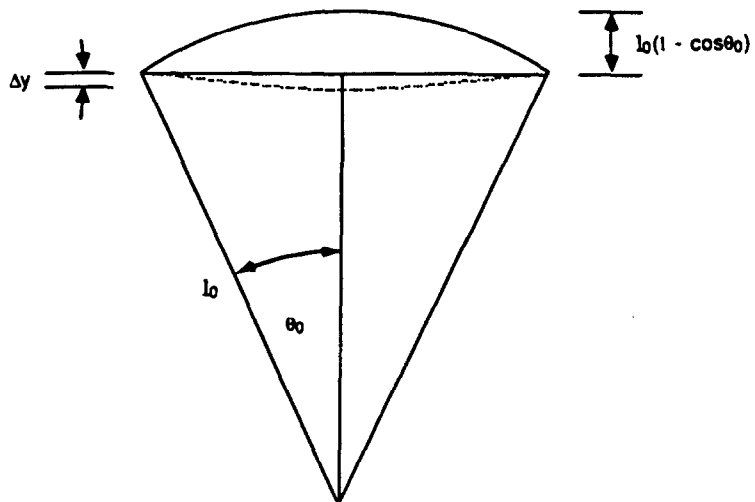


Fig. 9. Schematic drawing showing the trajectory of the mass (dotted curve), the vertical displacement of the mass at mid-step ( $\Delta y$ ) and other dimensions.

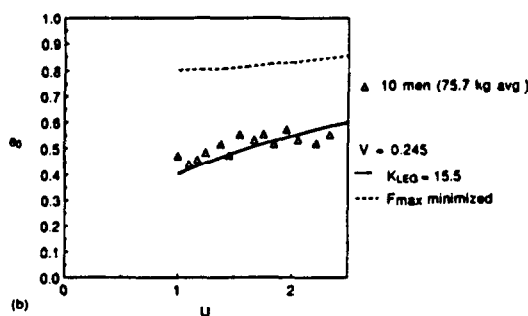
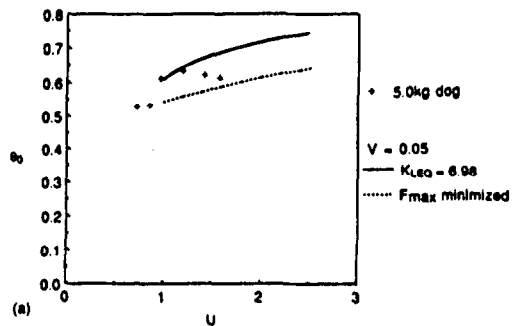


Fig. 10. Contrasting two alternative strategies for running. (a) Small dog. The solid curve shows how  $\theta_0$  would increase with  $U$  if  $K_{\text{LEG}}$  were fixed at 6.98 and  $V = 0.05$ . The broken curve, from Fig. 5(c), shows how  $\theta_0$  would increase with  $U$  if  $F_{\text{max}}/mg$  were minimized and  $V = 0.05$ . Crosses show results for a 5 kg dog trotting, calculated from Cavagna *et al.* (1988); (b) men. Solid curve shows  $K_{\text{LEG}}$  fixed at 15.5; broken curve shows  $F_{\text{max}}/mg$  minimized.

parameters  $U$ ,  $V$ , and  $\theta_0$  for bipeds running and quadrupeds trotting. The stride length  $s$  is defined as the distance between footprints of the same foot, and therefore includes the distance moved during both aerial phases and both contact phases of a single stride cycle.

Figure 9 is a schematic diagram used later. In Fig. 10, data for  $\theta_0$  are given for a dog trotting and men running. These data are compared with two paradigms for running, constant leg stiffness (solid curve) and minimum vertical force (broken curve). In Fig. 11, the dimensionless leg stiffness is assumed to be fixed at  $K_{\text{LEG}} = 15$ ,  $V$  is held constant at 0.18, and the predictions for relative stride length  $S = s/L_0$  vs  $U$  and  $\theta_0$  vs  $U$  are compared with values calculated from published measurements.

## DISCUSSION

### *Is the leg-spring model plausible?*

Since the undamped spring model presented in this paper makes several predictions that are testable by experiment, it is useful to review the plausibility of the model in light of comparisons with published experimental results.

Firstly, the generally good agreement between the experimental records of vertical acceleration vs vertical displacement and calculated simulations of the same records (Fig. 6) lend support to the validity of the model. It is true that the experimental record for the man running shows an early rise in vertical force, followed by a fall, before a rise to a second peak at mid-step, and this feature is not predicted by the model. There is evidence (McMahon *et al.*, 1987) that the early peak is due to the rapid deceleration of the mass of the foot and shank as it strikes the ground, a feature not represented in the present model.

The experimental records for both the man and the kangaroo (Fig. 1) show that take-off occurs ( $A$ , reaches  $-1$  at the end of the contact period) when the mass is somewhat higher than it was on landing. This is a consistent feature of such records, and it is not represented in the present model, which presumes a symmetric landing and take-off.

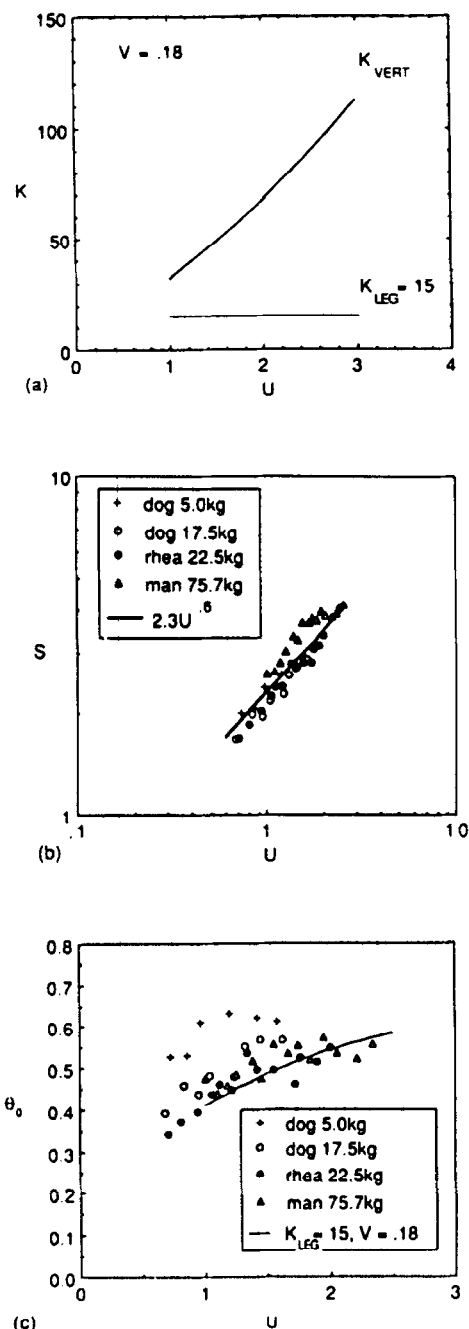


Fig. 11. Predictions of the model when  $V$  and  $K_{\text{LEG}}$  are fixed at values that best represent stride length information. (a)  $K_{\text{LEG}}$  does not vary with speed but  $K_{\text{VERT}}$  increases as  $U$  increases; (b)  $S = s/l_0$  is assumed to obey Alexander's relation  $S = 2.3U^{0.6}$  (solid line); (c) the predictions of the model for  $\theta_0$  (solid curve) compared with animal data. All animal points calculated from experimental results given by Cavagna *et al.* (1988).

A feature of the kangaroo simulation [Fig. 6(c)] is the 'stiffening' character of the vertical spring. At low force levels, the slope of the calculated curve in Fig. 6(c) is only about 43 % of the value it has at the highest force levels (mid-step). The experimental curve characterizing the vertical spring in Fig. 1 reveals a

similar effect, since the slope for low force levels ( $0 > A, > -1$ ) is about half of the slope at high forces ( $A, > 2$ ). In the model, this property of the vertical spring must be attributed to interactions between geometry and dynamics, since the stiffness of the leg-spring itself is strictly independent of force level. The property of a stiffening vertical spring was found only in simulations where the initial leg angles were large, typically above 0.9 rad.

In a previous study from this group (McMahon *et al.*, 1987), it was found that men running normally at intermediate speeds preferred a contact-time phase parameter  $\omega_0 t_c$  near 4.2, but  $\omega_0 t_c$  increased, eventually approaching  $2\pi$ , as the subjects deliberately flexed their knees more to reduce the vertical stiffness of the legs. The star in Fig. 8(a) shows that the contact-time phase parameter  $\omega_0 t_c$  is predicted to be 4.21 when the input parameters are  $U = 1.6$ ,  $V = 0.245$ , and  $\theta_0 = 0.5$ , corresponding to the man in Table 1 running at  $18.0 \text{ km h}^{-1}$ . Thus the present model is in agreement with the previous experimental findings. In running with increased knee flexion, where  $\theta_0$  increases and  $V$  decreases, the present model predicts that  $\omega_0 t_c$  rises toward a limiting value of  $2\pi$ , as was observed experimentally.

#### Why is $K_{\text{LEG}}$ proportional to $U$ for fast running?

A significant feature of Fig. 4(b) is the nearly linear relationship between the required  $K_{\text{LEG}}$  (for a re-entrant running cycle using a particular  $V$  and  $\theta_0$ ) and the forward speed  $U$ , provided that  $U$  is greater than about 2.0. Another nearly linear relationship exists between  $K_{\text{LEG}}$  and  $V$  [Fig. 4(a)]. As shown in Fig. 5,  $f_{\text{max}}/mg$  is also linear in  $U$  and  $V$  for  $U > 2.0$ . Why should this be so?

A plausible explanation depends on the nearly flat trajectory followed by the mass during the contact period. An argument is given in Appendix D based on the approximation that the mass follows a perfectly level trajectory during contact. Setting the vertical impulse due to the ground reaction force equal to the weight of the mass times the contact period plus the change in vertical momentum gives the following expression for the leg-spring stiffness:

$$K_{\text{LEG}} = UV/C[\sin \theta_0(1 - \cos \theta_0)] + 1/C(1 - \cos \theta_0). \quad (3)$$

Here  $C$  is a constant dependent on the shape of the curve showing vertical force against time. (For the range of parameters corresponding to fast mammalian terrestrial locomotion,  $C$  is close to 0.6.) Also given in Appendix D is an empirical formula based on corrections to the above equation. The empirical formula is capable of giving a value for  $K_{\text{LEG}}$  as a function of  $U$ ,  $V$ , and  $\theta_0$  that matches the value obtained from the numerical simulation to within about 0.5 % over the following range of input parameters:  $0 < V < 0.8$ ;  $5 < U < 30$ ;  $0.4 < \theta_0 < 0.8$ . Another set of empirical

formulae valid over the lower speed range  $0 < V < 0.3$ ;  $1 < U < 3$ ;  $0.4 < \theta_0 < 0.8$ , is given also.

Thus, the fact that  $K_{LEG}$  increases nearly linearly with both  $U$  and  $V$  for moderate and high values of  $U$  is a consequence of the nearly flat trajectory followed by the mass during contact. For a level trajectory, the maximum compression of the spring at mid-step is fixed by the choice of  $\theta_0$ . It follows that, for a given  $\theta_0$ , the maximum force is proportional to  $K_{LEG}$  when the mass follows a level trajectory, and since  $K_{LEG}$  increases linearly with  $U$  and  $V$ , so does  $f_{max}/mg$ , as was seen in Fig. 5(a).

All this applies for values of  $U$  greater than about 2.0. For  $U < 2.0$ , Figs 4(b) and 7(a) show that  $K_{LEG}$  falls below the extrapolated straight-line result valid for large  $U$ . Any curve showing  $K_{LEG}$  vs  $U$  does not go through the origin. There is a minimum value for  $K_{LEG}$ , and therefore a minimum value for  $U$ , for every pair of values for  $V$  and  $\theta_0$ . We remarked earlier as we introduced the dimensionless stiffness  $K_{LEG}$  (under Methods) that if  $\theta_0$ ,  $U$ , and  $V$  were all equal to zero and the leg-spring were pre-compressed until the spring force matched the weight, then the minimum value for  $K_{LEG}$  in this static, vertical geometry would be 1.0. When the leg begins from an incompressible state and when  $\theta_0$ ,  $U$ , and  $V$  are not zero, the minimum value for  $K_{LEG}$  will be greater than 2.0. In Fig. 7(a), simulating the man, we found that the lowest value of  $U$  which allowed the simulation to converge to a solution was  $U = 0.47$  corresponding to a  $K_{LEG} = 2.29$ . Any lower value of  $U$  caused the mass to strike the ground.

#### Why is $K_{VERT}$ greater than $K_{LEG}$ ?

One of the most important results of this paper is shown in Fig. 7(a). There it is demonstrated for input parameters representative of a man running that  $K_{VERT}$  is greater than  $K_{LEG}$  even for small values of  $U$ , and the two diverge very far from one another as  $U$  increases.

A physical explanation for the difference between  $K_{VERT}$  and  $K_{LEG}$  can be based on Fig. 9. The broken curve shows the trajectory of the mass during the contact period. Consider the instant at mid-step when the leg is vertical and has length  $(l_0 \cos \theta_0 - \Delta y)$ . At this instant, the vertical force is  $f_{max}$ . Thus the two stiffnesses are:

$$K_{VERT} = k_{vert} l_0 / mg = (f_{max} / mg) / (\Delta y / l_0) \quad (4)$$

and

$$K_{LEG} = k_{leg} l_0 / mg = (f_{max} / mg) / [1 - \cos \theta_0 + (\Delta y / l_0)]. \quad (5)$$

so that, for any finite value of  $\theta_0$ ,  $K_{VERT} > K_{LEG}$ .

In Fig. 7(b),  $K_{VERT}$  was found to be a nearly linear function not of  $U$  but of  $U^2$ , provided that  $U$  was greater than approximately 2.0. A simple argument can be given to understand the quadratic dependence. Suppose that a contact period occupies a given frac-

tion  $Q$  of a complete cycle of vertical vibration, so that

$$\omega_0 t_c = 2\pi Q, \quad (6)$$

where  $Q$  is assumed to be a constant. (For a given  $V$  and  $\theta_0$ , this assumption becomes more reasonable the higher the value of  $U$ , as was shown in Fig. 8(b).) Squaring both sides, substituting  $\omega_0^2 = k_{vert}/m$ , and solving for  $t_c^2$  gives

$$t_c^2 = 4\pi^2 Q^2 m / k_{vert}. \quad (7)$$

If we assume that fluctuations in horizontal speed of the mass are small during contact, the horizontal speed at impact  $u$  is about the same as the average horizontal speed during contact. Therefore,

$$u^2 = 4l_0^2 \sin^2 \theta_0 / t_c^2. \quad (8)$$

Solving (7) for  $k_{vert}$  and using (8) we obtain

$$k_{vert} = \pi^2 Q^2 m u^2 / l_0^2 \sin^2 \theta_0. \quad (9)$$

and since  $u^2 = U^2 g l_0$ , the dimensionless vertical stiffness is

$$K_{VERT} = \pi^2 Q^2 U^2 / \sin^2 \theta_0, \quad (10)$$

so that  $K_{VERT}$  is predicted to be a quadratic function of  $U$ , as the simulation showed.

An empirical formula, in which  $K_{VERT}$  is again a quadratic function of  $U$ , is given in equation (D12) of Appendix D. This formula, valid for the higher speeds, gives values for  $K_{VERT}$  as a function of  $U$ ,  $V$ , and  $\theta_0$  that generally are within 0.5% of the results of the numerical simulation within the stated range of input parameters. Another set of formulae, valid for lower values of  $U$ , appears at the end of Appendix D.

#### Longer steps at higher speeds

When the assumptions of the simulation kept both  $V$  and  $\theta_0$  fixed as  $U$  was increased, we found that the stride length predicted by the model was unrealistically large at low forward speeds. To make an improvement, we elected to specify the model in such a way that  $\theta_0$  increases as  $U$  increases. Two schemes are available to do this, one minimizing the peak force and the other keeping the leg stiffness fixed.

*Choosing a paradigm.* In Fig. 10(a), data are plotted showing  $\theta_0$  vs  $U$  for the 5.0 kg dog studied by Cavagna *et al.* (1977, 1988). We calculated  $\theta_0$  from the measurements published by these authors giving aerial time and stride length as a function of forward speed during trotting. We obtained the original films from the authors and made our own measurements of leg length  $l_0$ , averaging the values at toe-on and toe-off. The solid curve on the figure shows the prediction of the model for  $\theta_0$  when  $K_{LEG}$  is fixed at 6.98 and  $V = 0.05$  (Table 1). The broken curve shows the prediction from Fig. 5(c) when  $V = 0.05$  and  $\theta_0$  increases with  $U$  in such a way as to minimize  $f_{max}/mg$ . The data in Fig. 10(a) fall generally in the (narrow) space between the two curves. From this, we cannot decide whether it is more likely that the dog is following the constant

leg-stiffness or the minimum-force paradigm, since Fig. 10(a) could be used to support either hypothesis.

In Fig. 10(b), data for the average results of 10 men are compared with the two curves predicted by the model, that minimizing the peak vertical force (broken curve), and that for a fixed  $K_{\text{LEG}}$  (solid). In this figure, the solid curve represents the particular choices for  $K_{\text{LEG}}$  and  $V$  used in Table 1 to simulate a man running at  $18.0 \text{ km h}^{-1}$ . Two points are worthy of note. The first is that the broken curve is now above the solid curve, which is opposite from the order in Fig. 10(a). The second is that the points fall closer to the solid curve, and are therefore in better agreement with the paradigm of constant leg stiffness than that minimizing peak vertical force.

*Is constant  $K_{\text{LEG}}$  a reasonable assumption?* It is easy to visualize real physical circumstances corresponding to those simulated in Fig. 10, where leg stiffness remains fixed as speed increases. Alexander (1988) has pointed out that when the length of the Achilles tendon is much longer than the length of the muscle fibers in series with the tendon, the compliance (1/stiffness) of the tendon may be larger than that of the muscle, so that the stiffness of the leg may be determined by the stiffness of the tendon. If, as Alexander's argument suggests, this is true of the leg of a trotting dog, then the leg stiffness would not be expected to change much with speed because the stiffness of the tendon is about constant at moderate and high force levels.

Two other studies give evidence supporting the assumption of constant leg stiffness. In experiments using decerebrate cats, hindlimb stiffness was measured as the soleus muscle was forcibly lengthened by a small stretch (Hoffer and Andreassen, 1981). The overall stiffness, including that contributed by the stretch reflex, was found to vary only slightly with force at moderate and high force levels. In studies of human subjects bearing weights on their shoulders while standing on a springboard with knees flexed at a constant angle, it was found that the stiffness of the antigravity muscles including reflexes varied by less than 10% as the weight on the shoulders went from zero to more than twice body weight (Greene and McMahon, 1979b). It is interesting to note that if the simulations of Fig. 10(a) did indeed represent a dog trotting at various speeds, the forward speed could change by a factor of 2.2, from  $4.0$  to  $8.7 \text{ km h}^{-1}$ , and the vertical stiffness  $k_{\text{vert}}$  could increase by a factor of 3.58, from  $2.88$  to  $10.3 \text{ kN m}^{-1}$  while the leg stiffness remained fixed at  $K_{\text{LEG}} = 6.98$ , corresponding to  $k_{\text{leg}} = 1.49 \text{ kN m}^{-1}$ .

The ingenious running robots built by Marc Raibert and his group (Raibert, 1986) have legs that contain pneumatic springs in series with hydraulic actuators, so that the stiffness of the leg does not change much as speed is increased. Hence, evidence exists, in the form of a legged robot, that running faster without increasing the stiffness of the legs is a

practical strategy. The question remains: is this what animals do?

*Fixing the parameters of the constant- $K_{\text{LEG}}$  model.* In Fig. 11, the parameters of the model have been fixed in such a way as to give the best prediction of stride length as a function of speed for all the animals considered. As shown in Fig. 11(a),  $K_{\text{LEG}}$  has been set at the value 15.0, and  $V$  is constant at 0.18. The justification for fixing  $V$  is that when  $V$  is independent of the running condition, the distance the center of mass falls during an aerial phase is a given fraction of the leg length. If the legs are to clear the ground at both low and high forward speeds, it is reasonable to require that the body rises and falls a distance proportional to the leg length.

Alexander *et al.* (1977) recommended an empirical power-law function  $S = 2.3U^{0.6}$  to represent data he obtained for walking, trotting, and galloping animals of a range of sizes and speeds. Since that formula also fits the data (not Alexander's) plotted in Fig. 11(b), we elected to use the same formula and equation (C2) to find a set of paired values for  $\theta_0$  and  $U$  that was also compatible with a constant  $K_{\text{LEG}}$  and constant  $V$ . The result, which was obtained by iteration on  $V$ , is plotted in Fig. 11(c).

*A test of the model.* Since experimental data for  $\theta_0$  as a function of  $U$  were not used to formulate or specify the model, Fig. 11(c) may be regarded as a test of the theory. Agreement is quite good, particularly for the larger animals. A trend is apparent in the figure: the smaller the animal, the more its data points tend to lie above the curve. The fact that the smaller animals tend to swing their legs through larger excursion angles is a regular feature of animal scaling mentioned previously by McMahon (1975).

In summarizing Fig. 11, we can say that a model for terrestrial running based on the idea that the leg is a spring of constant stiffness is able to account for the way in which both stride length and step length increase with speed for bipeds running and quadrupeds trotting. Faster speeds are achieved by taking somewhat longer steps [Fig. 11(c)], and the longer steps give rise to a higher vertical stiffness [Fig. 11(a)] and consequently a shorter contact time. The longer stride length at higher speed [Fig. 11(b)] is determined by a greater distance moved during both the contact and the flight phases.

*What experimental measurements would be required to calculate  $K_{\text{VERT}}$  and  $K_{\text{LEG}}$ ?*

We conclude with a short discussion about how experimental observations of running may be used to calculate both the effective vertical stiffness, and, since this has more physiological relevance, the stiffness of the leg-spring. There are three ways to calculate  $k_{\text{vert}}$ . The three methods give answers which are not identical, but are the same to within a few per cent when applied to most of the parameter range of the model

of the present paper utilizing a frictionless, linear leg-spring.

(1)  $F_{\max}$ -and- $\Delta y$  method. This method was explained in connection with Fig. 6 and the definition of  $k_{\text{vert}}$ . The peak vertical force is divided by the downward displacement of the center of mass from foot strike to mid-step. The accuracy of this method is greatest when the segment of the force-displacement curve corresponding to contact is nearly linear, as it was in Fig. 6(b).

(2) Half-period method. Assume that the shape of the experimental vertical force record is sinusoidal (even for the simulation, it is not strictly sinusoidal unless there is no forward motion). Measure the time between the moment of zero vertical acceleration (vertical force =  $mg$ ) when the body is moving down and the moment of zero vertical acceleration when the body is moving up. Take this to be the half-period of vertical vibration  $P/2$  and calculate  $k_{\text{vert}} = m(2\pi/P)^{1/2}$ . This method was first used by Cavagna *et al.* (1988).

(3) Groucho method. Both of the above methods require a force plate capable of measuring the vertical force during a step. A third method, explained in McMahon *et al.* (1987), requires only a knowledge of the total body mass  $m$ , the contact time  $t_c$  and the time in the air  $t_a$ . The result may be stated:

$$k_{\text{vert}} = m\omega_0^2, \quad (11)$$

with

$$\tan(\pi - \omega_0 t_c/2) = \omega_0 t_a. \quad (12)$$

Relatively simple experiments may be all that is required to use one of the three methods above to determine  $k_{\text{vert}}$  for a given steady-speed running experiment. A central theme of this paper is that except for hopping in place, the stiffness of the leg is not the same thing as  $k_{\text{vert}}$ . How, then, should one estimate  $k_{\text{leg}}$  from experimental data?

A simple method is to use equation (5). The parameters needed are  $f_{\max}/mg$ ,  $\theta_0$ , and  $\Delta y/l_0$ , all of which are available from force-plate measurements, a knowledge of forward speed, and body dimensions.

**Acknowledgements**—The authors wish to thank R. McNeill Alexander, Reinhard Blickan, Bernard Budiansky, Norman Heglund, Richard Kronauer, and Marc Raibert for helpful discussions. We are grateful to Dr Heglund for making available to us original films he used in Cavagna *et al.* (1977). This research was supported by Grant number 86-10-9 from the Sloan Foundation.

#### REFERENCES

- Alexander, R. M. (1988) *Elastic Mechanisms in Animal Movement*. Cambridge University Press, U.K.  
 Alexander, R. M., Langman, V. A. and Jayes, A. S. (1977) Fast locomotion of some African ungulates. *J. Zool. Lond.* **183**, 291-300.

- Cavagna, G. A., Thys, H. and Zamboni, A. (1976) The sources of external work in level walking and running. *J. Physiol. Lond.* **262**, 639-657.  
 Cavagna, G. A., Heglund, N. C. and Taylor, C. R. (1977) Mechanical work in terrestrial locomotion: two basic mechanisms for minimizing energy expenditure. *Am. J. Physiol.* **233**, R243-R261.  
 Cavagna, G. A., Franzetti, P., Heglund, N. C. and Willems, P. (1988) The determinants of the step frequency in running, trotting and hopping in man and other vertebrates. *J. Physiol.* **399**, 81-92.  
 Greene, P. R. and McMahon, T. A. (1979a) Running in circles. *The Physiologist* **6**, S35-36.  
 Greene, P. R. and McMahon, T. A. (1979b) Reflex stiffness of man's anti-gravity muscles during knee bends while carrying extra weights. *J. Biomechanics* **12**, 881-891.  
 Hoffer, J. A. and Andreassen, S. (1981) Regulation of soleus muscle stiffness in premammillary cats: intrinsic and reflex components. *J. Neurophysiol.* **45**, 267-285.  
 McMahon, T. A. (1975) Using body size to understand the structural design of animals: quadrupedal locomotion. *J. appl. Physiol.* **39**, 619-627.  
 McMahon, T. A. (1985) The role of compliance in mammalian running gaits. *J. exp. Biol.* **115**, 263-282.  
 McMahon, T. A. (1987) Compliance and gravity in running. In *Biomechanics of Normal and Prosthetic Gait* (Edited by Stein, J. L.), Vol. 4, pp. 31-37. ASME.  
 McMahon, T. A., Valiant, G. and Frederick, E. C. (1987) Groucho running. *J. appl. Physiol.* **62**, 2326-2337.  
 Press, W. H., Flannery, B. P., Teukolsky, S. A. and Vetterling, W. T. (1986) *Numerical Recipes: the Art of Scientific Computing*. Cambridge University Press, New York.  
 Raibert, M. H. (1986) *Legged Robots that Balance*. MIT Press, Cambridge, MA.

#### APPENDIX A: HOPPING IN PLACE

In Fig. 2(a), the displacement  $y$  of the mass is measured upward. The spring is slack when  $y = 0$ . The vertical velocity  $dy/dt$  at the moment the leg-spring strikes the ground is  $-v$ , where  $v$  is a positive quantity. Because energy is conserved during the rebound from the ground, the take-off velocity at the end of the rebound is  $v$ . The equation of motion may be written in the form:

$$d^2 Y_1/dT_1^2 = -(Y_1 + 1), \quad (A1)$$

where the following dimensionless variables have been used,

$$Y_1 = (k_{\text{vert}}/mg)y, \quad (A2)$$

$$T_1 = \omega_0 t, \quad (A3)$$

and where  $t$  is time in seconds and

$$\omega_0 = (k_{\text{vert}}/m)^{1/2}. \quad (A4)$$

The initial conditions on the vertical displacement and velocity are

$$Y_1(0) = 0 \quad (A5)$$

and

$$dY_1/dT_1(\text{at } T_1 = 0) = -v\omega_0/g. \quad (A6)$$

The solution of (A1) subject to conditions (A5) and (A6) is

$$Y_1 = -(v\omega_0/g) \sin T_1 - (1 - \cos T_1). \quad (A7)$$

Since the vertical force  $f_y$  applied by the spring to the mass is

$$f_y = -k_{\text{vert}}y = -mgY_1, \quad (A8)$$

the vertical force normalized by the weight  $mg$  is

$$F_y/f_y = mg = (v\omega_0/g) \sin T_1 + 1 - \cos T_1. \quad (A9)$$

The phase  $T_{1(\text{maxforce})}$ , at which  $F$  reaches a maximum value is found by differentiating (A9) and equating to zero, giving

$$T_{1(\text{maxforce})} = \tan^{-1}(-v\omega_0/g) = \pi - \tan^{-1}(v\omega_0/g). \quad (\text{A10})$$

The peak force  $F_{\text{max}}$  occurs midway through the contact period, at  $T_{1(\text{maxforce})}$ . Thus

$$F_{\text{max}} = (v\omega_0/g) \sin T_{1(\text{maxforce})} + 1 - \cos T_{1(\text{maxforce})}, \quad (\text{A11})$$

and the dimensionless period of contact  $T_{1(\text{endcontact})}$  is

$$T_{1(\text{endcontact})} = \omega_0 t_c = 2T_{1(\text{maxforce})} = 2\pi - 2 \tan^{-1}(v\omega_0/g). \quad (\text{A12})$$

The time spent in the air during one aerial phase is

$$t_{\text{aerial}} = 2v/g, \quad (\text{A13})$$

giving a dimensionless aerial time of

$$T_{1(\text{aerial})} = 2v\omega_0/g. \quad (\text{A14})$$

For a biped hopping in place on both legs, a complete hop is one contact phase and one aerial phase. The stride frequency is defined to be  $f_s$ , measured in hops per second. Given in dimensionless terms, it is

$$\phi_s = f_s/\omega_0 = 1/(T_{1(\text{endcontact})} + 2v\omega_0/g), \quad (\text{A15})$$

where  $T_{1(\text{endcontact})}$  is given by (A12). Since both terms within the parentheses of (A15) are determined by  $v\omega_0/g$ , there is a unique relationship between  $\phi_s$  and  $v\omega_0/g$ . At low values of  $v\omega_0/g$ ,  $\phi_s$  is near  $2\pi$ . At large values of the Groucho number  $v\omega_0/g$ ,  $\phi_s$  tends toward  $1/(2v\omega_0/g)$ , so that the dimensionless stride frequency  $\phi_s$  approaches zero.

When an animal runs in place, hopping on first one leg and then the other, the total stride period is the time to complete two hops, so that the stride frequency is half of that given by (A15).

## APPENDIX B: HOPPING OR RUNNING FORWARD

The variables  $l$ ,  $l_0$ ,  $x$ ,  $y$ ,  $\theta$ , and  $\theta_0$  are defined in Fig. 2(b). The equations of motion are

$$d^2X/dT^2 = K_{\text{LEG}}(1-L) \sin \theta \quad (\text{B1})$$

and

$$d^2Y/dT^2 = K_{\text{LEG}}(1-L) \cos \theta - 1 \quad (\text{B2})$$

with

$$X = x/l_0; \quad Y = y/l_0; \quad L = l/l_0, \quad (\text{B3})$$

$$T = t(g/l_0)^{1/2} \quad (\text{B4})$$

and

$$K_{\text{LEG}} = k_{\text{leg}}l_0/mg. \quad (\text{B5})$$

The initial and final conditions are

$$\theta(T=0) = -\theta_0, \quad (\text{B6})$$

$$\theta(T=T_{\text{endcontact}}) = \theta_0, \quad (\text{B7})$$

$$L(T=0) = L(T=T_{\text{endcontact}}) = 1, \quad (\text{B8})$$

$$dX/dT(T=0 \text{ and } T=T_{\text{endcontact}}) = u/(gl_0)^{1/2} = U, \quad (\text{B9})$$

$$dY/dT(T=0) = -v/(gl_0)^{1/2}, \quad (\text{B10})$$

and

$$dY/dT(T=T_{\text{endcontact}}) = v/(gl_0)^{1/2} = V. \quad (\text{B11})$$

## APPENDIX C: STRIDE LENGTH AND STRIDE FREQUENCY

For any animal gait, the distance between footprints of the same foot is called the *stride length*. When a biped runs or a

quadruped trots, the distance moved forward during one contact period is  $2l_0 \sin \theta_0$  and the distance moved forward during one aerial phase is  $2v\omega_0/g$ . Doubling these distances to get the distance moved forward during one stride cycle, the stride length  $s$  is

$$s = 4l_0 \sin \theta_0 + 4v\omega_0/g. \quad (\text{C1})$$

Defining the dimensionless or relative stride length as  $S = s/l_0$ ,

$$S = s/l_0 = 4(\sin \theta_0 + UV). \quad (\text{C2})$$

Provided that the fluctuations in forward speed during contact are small, the speed at contact  $u$  can give a good approximation of the average forward speed during a stride cycle. If this is true, then the stride frequency  $f_s$  for bipeds running and quadrupeds trotting is

$$f_s = u/s = u/(4l_0 \sin \theta_0 + uv/g), \quad (\text{C3})$$

so that the dimensionless stride frequency  $\phi_s$  is

$$\phi_s = f_s/(g/l_0)^{1/2} = U/4(\sin \theta_0 + UV). \quad (\text{C4})$$

## APPENDIX D: APPROXIMATE $K_{\text{LEG}}$ FOR A FLAT TRAJECTORY

Suppose the mass follows a flat trajectory during the contact period. As shown in Fig. 9, the maximum compression of the leg-spring at mid-step is  $l_0(1 - \cos \theta_0)$ . Thus, the maximum vertical force at mid-step is

$$f_{\text{max}} = k_{\text{leg}}l_0(1 - \cos \theta_0). \quad (\text{D1})$$

The vertical impulse is the area under the curve showing vertical force vs time. An approximation of this vertical impulse is

$$\text{Impulse} = mgT_c + 2mv \approx Cf_{\text{max}}T_c. \quad (\text{D2})$$

Assuming that the forward speed  $u$  is nearly steady,

$$u \approx s/t_c = 2l_0 \sin \theta_0/t_c. \quad (\text{D3})$$

Solving (D1) for  $k_{\text{leg}}$  and using (D2), (D3),  $K_{\text{LEG}} = k_{\text{leg}}l_0/mg$  and  $uv = UV/gl_0$ ,

$$K_{\text{LEG}} = UV/C[\sin \theta_0(1 - \cos \theta_0)] + 1/C(1 - \cos \theta_0). \quad (\text{D4})$$

### Empirical formulae: high speed

The following empirical formulae give the same results as the numerical simulations to within 0.5% over the high-speed range  $5 < U < 30$ ;  $0 < V < 0.8$ ;  $0.4 < \theta_0 < 0.8$ .

$$K_{\text{LEG}} = HU + J, \quad (\text{D5})$$

with

$$H = 2.0V/[\sin \theta_0(1 - \cos \theta_0)N], \quad (\text{D6})$$

$$N = 1.423 - 0.309\theta_0, \quad (\text{D7})$$

$$J = 2.0/(1 - \cos \theta_0) - P, \quad (\text{D8})$$

$$P = Q\theta_0 - R, \quad (\text{D9})$$

$$Q = 0.616 + 1.629V + 4.051V^2, \quad (\text{D10})$$

$$R = 2.610 + 1.397V - 0.924V^2. \quad (\text{D11})$$

Over the same range,  $K_{\text{VERT}}$  may be found from:

$$K_{\text{VERT}} = (AU + B)^2, \quad (\text{D12})$$

with

$$A = 1.788(\theta_0)^{-0.888}, \quad (\text{D13})$$

$$B = 5.905(10)^{-1.552V}. \quad (\text{D14})$$

### Empirical formulae: low speed

At low speeds,  $K_{\text{LEG}}$  and  $K_{\text{VERT}}$  are no longer nearly linear functions of  $U$  and  $V$ . The following expansions give the same

results as the numerical simulations to within 0.5 % over the range  $1 < U < 3$ ,  $0 < V < 0.3$ ,  $0.4 < \theta_0 < 0.8$ .

$$K_{\text{LEG}} = A(\theta_0) + B(\theta_0)U + C(\theta_0)U^2 + D(\theta_0)U^3$$

$$A(\theta_0) = A_0 + A_1\theta_0 + A_2\theta_0^2 + A_3\theta_0^3 + A_4\theta_0^4 + A_5\theta_0^5$$

$$B(\theta_0) = B_0 + \dots$$

$$C(\theta_0) = C_0 + \dots$$

$$D(\theta_0) = D_0 + \dots$$

$$K_{\text{VERT}} = A(\theta_0) + B(\theta_0)U + C(\theta_0)U^2$$

$$A(\theta_0) = A_0 + A_1\theta_0 + A_2\theta_0^2 + A_3\theta_0^3 + A_4\theta_0^4 + A_5\theta_0^5$$

$$B(\theta_0) = B_0 + \dots$$

$$C(\theta_0) = C_0 + \dots$$

V	Coef. No.	Coef. No.				A	B	C
		A	B	C	D			
0.00	0	70.512	96.100	-35.3560	4.3960	0.00	0	-104.710
0.00	1	-392.550	-453.710	160.5100	-18.9190	0.00	1	789.040
0.00	2	958.230	940.970	-316.4100	34.5900	0.00	2	-2422.500
0.00	3	-1232.100	-986.910	307.9500	-29.6310	0.00	3	3596.100
0.00	4	814.150	505.330	-139.4200	10.1590	0.00	4	-4592.700
0.00	5	-219.780	-95.134	19.9910	-0.2118	0.00	5	-718.850
0.05	0	32.846	129.870	-30.0300	3.5513	0.05	0	-32.194
0.05	1	-192.920	-626.560	122.0800	-13.4340	0.05	1	-193.550
0.05	2	516.340	1307.400	-204.5700	19.6910	0.05	2	1054.500
0.05	3	-742.040	-1367.600	141.7700	-8.3794	0.05	3	-1892.400
0.05	4	548.870	689.190	-13.9070	-5.6238	0.05	4	1504.000
0.05	5	-165.600	-124.570	-18.4490	4.6271	0.05	5	-454.660
0.10	0	-3.170	163.210	-27.7880	3.1094	0.10	0	-25.896
0.10	1	9.725	-812.680	106.7900	-10.2620	0.10	1	183.480
0.10	2	48.062	1724.600	-150.8100	8.6397	0.10	2	129.070
0.10	3	-210.060	-1811.100	38.3280	12.0240	0.10	3	-193.550
0.10	4	260.470	898.980	84.5890	-24.2430	0.10	4	-789.900
0.10	5	-108.660	-153.800	-54.7150	11.2350	0.10	5	-201.810
0.15	0	-8.564	158.290	-8.3556	0.6799	0.15	0	-15.986
0.15	1	19.151	-771.390	-15.3730	4.5254	0.15	1	-746.630
0.15	2	57.831	1625.500	159.2800	-27.6950	0.15	2	-154.480
0.15	3	-250.360	-1713.200	-356.4800	56.7330	0.15	3	-2349.000
0.15	4	300.730	860.780	337.0400	-51.8810	0.15	4	-106.330
0.15	5	-123.450	-149.660	-120.1500	18.2000	0.15	5	-297.130
0.20	0	-27.482	166.400	-3.0621	0.4582	0.20	0	10.661
0.20	1	151.940	-849.670	-20.4160	1.2781	0.20	1	99.079
0.20	2	-345.580	1921.000	96.8780	-7.1177	0.20	2	-562.690
0.20	3	371.770	-2236.200	-173.5500	13.6310	0.20	3	685.380
0.20	4	-175.750	1298.800	149.3700	-12.8800	0.20	4	1124.500
0.20	5	19.743	-289.170	-53.4380	5.2200	0.20	5	-201.810
0.25	0	-85.256	223.170	-12.1260	1.7650	0.25	0	144.150
0.25	1	620.740	-1345.600	94.2170	-14.6110	0.25	1	-302.930
0.25	2	-1869.600	3603.800	-356.7700	54.9920	0.25	2	-776.040
0.25	3	2810.100	-5003.100	636.8400	-96.8440	0.25	3	-113.270
0.25	4	-2087.800	3508.800	-531.5300	79.8460	0.25	4	-180.600
0.25	5	606.420	-975.790	165.1400	-24.5580	0.25	5	164.260
0.30	0	29.796	39.120	113.0800	-18.1840	0.30	0	-2117.700
0.30	1	-391.900	236.850	-962.7800	155.7200	0.30	1	-184.780
0.30	2	1594.800	-1753.300	3195.8000	-521.8400	0.30	2	1306.100
0.30	3	-2992.300	3923.000	-5267.4000	866.9800	0.30	3	-290.620
0.30	4	2682.600	-3812.800	4310.8000	-713.8700	0.30	4	103.340
0.30	5	-937.130	1391.700	-1402.6000	233.2500	0.30	5	-440.380